Travelling fire experiments in steel-framed structure: numerical investigations with CFD and FEM

Travelling fire experiments in steel-framed structure: numerical investigations with CFD and FEM

Marion Charlier [(1*)], Antoine Glorieux [(2)], Olivier Vassart [(3)], Xu Dai [(4)], Stephen Welch [(5)], Johan Anderson [(6)], Ali Nadjai [(7)]

[(1)] ArcelorMittal Global R&D, marion.charlier@arcelormittal.com
66 rue de Luxembourg L-4221 Esch/Alzette, Luxembourg
https://orcid.org/0000-0001-7690-1946

[(2)] ArcelorMittal Global R&D, antoine.glorieux@arcelormittal.com
66 rue de Luxembourg L-4221 Esch/Alzette, Luxembourg
https://orcid.org/0000-0001-5982-0300

[(3)] ArcelorMittal Steligence, olivier.vassart@arcelormittal.com
https://orcid.org/0000-0001-5272-173X

[(4)] School of Engineering, The University of Edinburgh, x.dai@ed.ac.uk
https://orcid.org/0000-0002-9617-7681

[(5)] School of Engineering, The University of Edinburgh, s.welch@ed.ac.uk
https://orcid.org/0000-0002-9060-0223

[(6)] RISE Research Institutes of Sweden, johan.anderson@ri.se
https://orcid.org/0000-0001-7524-0314

[(7)] Ulster University, FireSERT, a.nadjai@ulster.ac.uk
https://orcid.org/0000-0002-9769-7363

* Corresponding author

Abstract

Purpose

The purpose of this paper is to propose a simplified representation of the fire load in CFD to represent the effect of large-scale travelling fire, and to highlight the relevance of such an approach while coupling the CFD results with FEM to evaluate related steel temperatures, comparing the numerical outcomes with experimental measurements.

Design/methodology/approach

This paper presents the setup of the CFD simulations (FDS software) and its corresponding assumptions, and the calibration of two natural fire tests while focusing on gas temperatures and on steel temperatures measured on a central column. For the latter, two methods are presented: one based on EN1993-1-2 and other linking CFD and FEM (SAFIR® software).

Findings

This paper suggests that such an approach can allow for both an acceptable representation of the travelling fire in terms of fire spread and steel temperatures. On the other hand, there are therefore inevitable limitations inherent to the simplifications made, these are also discussed. Regarding steel temperatures, the two methods lead to quite similar results, but with the ones obtained via CFD-FEM coupling closer to the ones measured.

Originality

This work has revealed that the proposed simplified representation of the fire load appears to be appropriate to evaluate the temperature of steel structural elements within reasonable limits on computational time, making it potentially desirable for practical applications. This paper also presents the first comparisons of FDS-SAFIR® coupling with experimental results, highlighting promising outcomes.

Key words

Travelling fire; Steel structure; CFD; FEM

Article classification

Research Paper

1. Introduction

The development of knowledge concerning the appropriate representation of the fire load for large compartments in CFD is required to be able to further analyze the influence of compartment geometry on the development of a travelling fire, and to perform numerical analyses of the temperature development. The coupling with FEM allows for assessing the mechanical behavior of structures that considers comprehensively the travelling nature of the fire. Within the context of the European RFCS TRAFIR project, a series of three natural fire tests were performed, involving a steel-framed structure and a continuous fuel bed made of several layers of wood sticks provided in three different directions (alternation of 60°-120°-180°) (Nadjai *et al.*, 2020). The aim of this experimental campaign was to perform uncontrolled tests based on a well-established fire load, to characterize the thermal impact generated by travelling fires, to evaluate the influence of the ventilation conditions on the development of the fire and to assess the fire impact on the steel structural elements. A parametrical study using the FDS software was conducted to calibrate the model using a simplified representation of the fire load. Simplifications were targeted, to afterwards enable reproduction of a broader range of scenarios encompassing different fires and end-use situations, so as to generate an extended virtual experimental dataset, as well as to facilitate analyses of real building dimensions.

The CFD simulations consider a simplified representation of the continuous fire load consisting of discrete volumes (cubes) based on a regular arrangement. The overall heat release rate per unit area curve is used as an input and the spread mechanism is determined using planar devices on each face of the cribs to measure the temperatures on the solid surfaces. If the surface temperature reaches the ignition temperature on at least one face of the volume, then all surfaces are set to start burning following the prescribed heat release rate per unit area curve.

A similar chessboard pattern was used by Horová (2015), to calibrate the Veselí fire test carried out in the Czech Republic in 2011 (F. Wald *et al*., 2011) launched in the frame of the European project COMPFIRE, having as the main objective to provide an integrated approach for the practical application of performance-based fire engineering design of composite structures. In the experimental campaign, the fire load was composed of wood sticks of dimensions 5 x 5 x 100 cm placed into 24 cribs. The total fire load consisted of 24 wood piles placed closely one to another, corresponding to a value of 198.4 MJ/m^2. Horová highlights that while adoption of wood cribs arranged into piles as fire load in the experiment seems to be very advantageous it causes significant drawback in mathematical modelling. Indeed, the small size of the sticks (by comparison with the compartment size) implies the definition of small cell size in the vicinity

of the fire load which results in very time consuming calculations. Horová therefore states that substituting highly resolved wood piles with a fictitious material of a simple geometry may lead to shorter computational times, and proposes a mass layers pattern consisting of blocks of wood with the layout of a chessboard, keeping properties and total dimension of the original wood crib as close as possible. This model was calibrated against the growing phase of the heat release rate curve and gas temperatures from the Veselí fire test (comparison is focused on distribution of gas temperature at the ceiling level). The calibration is focused on gas temperatures along the beams. Calculated gas temperatures reach slightly higher values in comparison with the measured values but the numerical model shows good agreement in the growing phase. A significant difference is observed for the descending phase.

Degler *et al.* (2015) used a similar pattern to perform *a priori* numerical analysis of the Tisova fire test (Czech Republic), which was performed to investigate the impact of a travelling fire on concrete and composite structures (Rush *et al*., 2016). A continuous fuel bed of 170 m^2 comprised of wood sticks and corresponding to a fire load of 680 MJ/m^2 was laid in a compartment of 230 m^2, part of a 4-storey concrete frame building. The aim of the numerical investigation was to perform *a priori* analyses of gas temperatures to be expected and to provide guidelines concerning the amount of fuel to be used in the test.

Charlier *et al.* (2018) used a similar approach to perform numerical works in the frame of the TRAFIR project to analyze the influence of compartment geometry and the interaction with representative fuel loads to explore the conditions leading to the development of a travelling fire. No comparison with an experimental campaign was performed, but the CFD results were used to perform numerical analyses of the temperature development and resulting mechanical behaviour of a theoretical steel structure using SAFIR® software.

The above mentioned findings highlight that adaptation is needed to represent the fire load, when structural analysis follows. Indeed, fire dynamics deals with a much smaller scale than the structural mechanics and yet these two sciences needs to be combined, requiring a simplified approach to model the fire load. This paper suggests that such an approach can allow for both an acceptable representation of the travelling fire in terms of fire spread & steel temperatures and an acceptable computational time. On the other hand, there are therefore inevitable limitations inherent to the simplifications made, and these are also discussed.

This paper presents the setup of the CFD simulations and its corresponding assumptions, and the calibration of two of the three TRAFIR natural fire tests. Gas temperatures measured at

mid-width, along the length of the compartment (at several levels) and the rate of heat release (evaluated through the mass loss recording on a central platform) are compared with the ones resulting from the CFD simulations. Furthermore, steel temperatures measured on a central steel column made of hot rolled profile are compared with the CFD results following two methods: one based on the incremental formula from EN1993-1-2 and other one linking CFD (FDS software) and FE (SAFIR software) following the weak coupling approach described by Tondini *et al.* (2016). In the fire engineering field, few applications of coupling CFD with FE are available. Wickström *et al.* (2007) presented a way of transferring to the thermal/structural model the description of the gas phase via the adiabatic surface temperature. The European RFCS project FIRESTRUC (Welch *et al*., 2008) dealt with studying different coupling approaches and using different software. Tondini *et al.* (2012) launched *a priori* simulations to model a steel rack system to be placed next to a pool fire and later, Tondini *et al.* (2016) described a comparison between the fire performance of a theoretical steel-concrete composite open car park (analysed while by applying the Hasemi model and the FDS–SAFIR integrated methodology). Charlier *et al.* (2018) applied the FDS–SAFIR integrated methodology to evaluate temperature development and resulting mechanical behaviour of a theoretical steel structure subjected to travelling fire. The present paper is the first to compare results from this FDS–SAFIR integrated methodology with experimental results.

2. Travelling fire tests in experimental steel building

The experimental campaign of the TRAFIR project aimed at performing large-scale tests in real building dimensions with no control over of the fire dynamics (Nadjai *et al.*, 2020). Three tests were planned:

- A fuel controlled travelling fire, referred as test n°1;
- A ventilation controlled fire intended to lead to a flashover, referred as test n°3:
- Another travelling fire, with less ventilation than in test n°1, referred as test n°2.

During these tests, gas temperatures, steel temperatures and mass loss rate were recorded, and this data serves as a basis for the calibration of CFD models.

2.1 Steel-framed structure and openings

For the natural fire tests, the compartment was designed to represent a part of an entire office layout, consisting of steel beams and columns for the main structural frame, while hollow-core precast slabs were used for the construction of the roof. The structure layout (see Figure 1- Layout plan of the test compartment and location of TRL4 to TRL8 (dimensions in mm))

and fire load (described below) were identical for the three tests. Only the opening layouts were modified, to assess the influence of the ventilation conditions on the development of the fire. The floor plan between the outer gridlines of the test structure was 15m x 9m and the level of the ceiling from the floor finish surface was 2.90 m. This paper considers tests n°1 and n°2.

For test n°1, a concrete wall was constructed along the shorter dimension of the compartment, along gridline 1. In addition to the back wall, down-stands were provided along the longer dimension of the compartment along gridlines A and B. Neither the wall nor the down-stands are present along the shorter dimension of the compartment, along gridline 4. The back wall is constructed using precast concrete, while the down-stands consist of two layers of gypsum fire boards having a thickness of 2 x 12.5 mm. The total surface area of openings is 85.2 m^2.

For test n°2, an additional concrete block wall was constructed along the other shorter dimension (along gridline 4). Furthermore, a 0.8 meter height concrete block soffit was constructed along the longer dimensions (gridlines A and D) such that the opening height is 1 meter along both longer sides of the compartment. This configuration results in openings with a total area of 30 m^2. These openings were equally distributed along gridlines A and D with an area of 15 m^2 each. Photographs of the test compartments can be seen on Figure 2 (a) and (b).

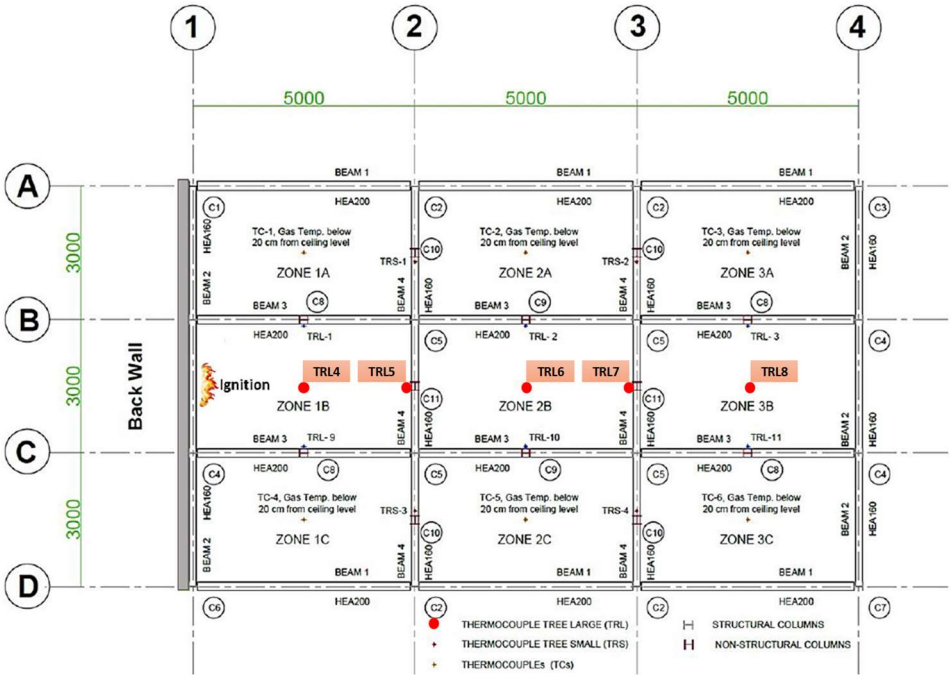

Figure 1- Layout plan of the test compartment and location of TRL4 to TRL8 (dimensions in mm)

Figure 2 - Photographs of the experimental campaign carried out by Ulster University in the frame of TRAFIR project: (a) compartment for test n°1 ; (b) compartment for test n°2 ; (c) continuous fire load made of wood sticks for test n°1 and test n°2 ; (d) fire at the beginning of test n°2

2.2 Fire load

Also in the frame of the TRAFIR project, Franssen *et al. (2019)* performed a series of fire tests with uniformly distributed cellulosic fire loads, aiming at defining an arrangement representative of an office building according to Eurocode 1 (CEN, 2002). This work led to devise a well-established methodology (Gamba *et al.,* 2020), used to define the fuel load

arrangement for the natural fire tests considered in this paper. The wood species consisted of *picea abies* with an average density of 470 kg/m^3. To achieve a medium fire growth rate, 9 layers of wood sticks with an axis distance of 120 mm (90 mm intervals) were provided in three different directions (alternation of 60°-120°-180°), as shown in Figure 2 (c), resulting in a fire load density of 511 MJ/m^2 (80% fractile, as given in EN1991-1-2 for an office building). The fuel bed was provided along the centre of the test compartment, in a rectangular band shape of 14 m long stretching from wall to wall along the longer dimension of the test compartment (a gap of 0.5 m was kept between the short walls and the edge of the fire load). The width of the fuel bed was 4.2 m and was aligned with the centreline of the compartment. The wood sticks were provided on a platform constructed using concrete blocks and gypsum fireboards: the top surface of the platform was placed at 325 mm from the floor finish level. For each test, the ignition was defined at a point located at mid-width of the fire load, 0.5 m from its edge (i.e. at a distance of 1 m from the back wall). The fire started to grow close to gridline 1 and then travelled from gridline 1 to gridline 4 (see Figure 2 (d)).

3. Modelling the experimental campaign through CFD

Several CFD simulations were launched with the FDS software (version 6.7.3) (McGrattan *et al.,* 2017) to calibrate the model for these natural fire tests, and the paper presents the comparison between numerical and experimental results in terms of gas and steel temperatures. Steel temperatures are computed using two different methods: using the incremental formula from EN1993-1-2 (CEN, 2005) and while coupling CFD and FEM. The CFD simulations consider a simplified representation of the continuous fire load consisting of discrete volumes (cubes) based on a regular arrangement (no detailed representation of a wood crib involving alternation of sticks and air gap was used here). Simplifications were targeted, as the modelling of the real wood stick size in CFD requires a very fine mesh and therefore a very significant computational time for real building geometries. Several parameters (FDS cell size, cubes size, ignition temperature, heat release rate per unit area and its evolution with time) were varied to reach the final CFD model presented below. These CFD simulations were launched on an HPC (High Performance Computing) cluster, and the simulations required 36.9 and 41.6 hours (for test n°1 and n°2, respectively) to complete using 24 cores (6 MPI processes with 4 OpenMP threads per process).

3.1 Computational domain and materials

The FDS domain's VENTs are all defined as OPEN, except the lower limit (representing the floor) which is set as INERT (the VENT group is used to prescribe planes adjacent to obstructions or external walls). The ceiling is made of 15 cm of concrete, and the short wall built along gridline 1 is represented as a succession of 3 layers: concrete (8 cm), insulation type 1 (10 cm) and concrete (15 cm). The insulation type 2 material is used to represent the down-stands (1,5 cm thickness) and the platform (3 cm thickness) on which the fire load lies. For test n°2, the additional soffit (along the longer dimension) is made of 15 cm of manufactured concrete blocks. Finally, the additional short wall (along gridline 4) is defined with two layers: 1.5 cm of insulation type 2 and 15 cm of manufactured concrete blocks. The thermal properties of the above-mentioned materials are described in Table I. As in the test, the platform on which the fire load lies is elevated from the floor. All the OBST's are less than or equal to one cell thick and the attached SURFs have a backing defined as "exposed" (i.e. the innermost layer is exposed to the air temperature on the back side). The domain size is 18.56m x 12.48m x 3.04m with cells of 0.16m x 0.16m x 0.16m, resulting in a total cell number equal to 171 912. The domain is divided into six meshes distributed along the length of the compartment (i.e. along gridlines A-B-C-D).

Table I – Thermal properties of the different materials defined in the CFD model

	Conductivity [W/m/K]	**Specific heat [kJ/kg/K]**	**Density [kg/m^3]**	**Emissivity [-]**
Concrete	1.6	1.0	2400	0.8
Insulation type 1	0.09	0.66	45	0.9
Insulation type 2	0.24	1.25	900	0.89
Manufactured concrete blocks	0.92	1.05	1973	0.8

3.2 A simplified representation of the fire load

The cell size used in the FDS models depends highly on the situation that is modelled and on the purpose of the simulation. Several attempts are considered: having cell size equal to 0.16 m or 0.32 m and cube size equal to 0.16 m, 0.32 m or 0.64m. Concerning the cube size, Horová (2015) advises to define cell size at least two times smaller than the object size. Indeed, no proper fire spread was achieved for the simulations where the cell size equals the cube size, as expected. The final calibrated model considers a 0.16m cell size and 0.32 m cube size, which lead to an acceptable computation time. The overall heat release rate was used as input to

VENTs, with each VENT representing a cube face (the lower face excluded). The wood constituting the cubes (*Picea abies*, the Norway spruce or European spruce) has the following chemical composition: $C_{1.0}H_{3.584}O_{1.55}$ with an assumed soot yield of 0.015 [g/g] (adopted from the SFPE Handbook (2002)) and a heat of combustion of 1.684 MJ/kg (obtained from a bomb calorimeter test conducted by the University of Edinburgh). The conductivity and the specific heat of the modelled wood vary with temperature (as adopted by Yang (2016)) and its density is approximately 468 kg/m^3 (measured by Liège University). The modelled compartment for tests n°1 and n°2 and the simplified fire load (which is identical for each) are depicted on Figure 3 and Figure 4 (a), respectively.

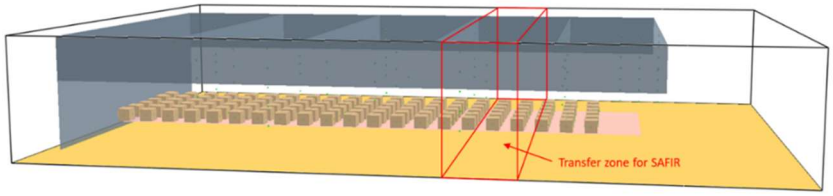

Figure 3 – FDS model for the fire test n°1 with the transfer zone for SAFIR highlighted

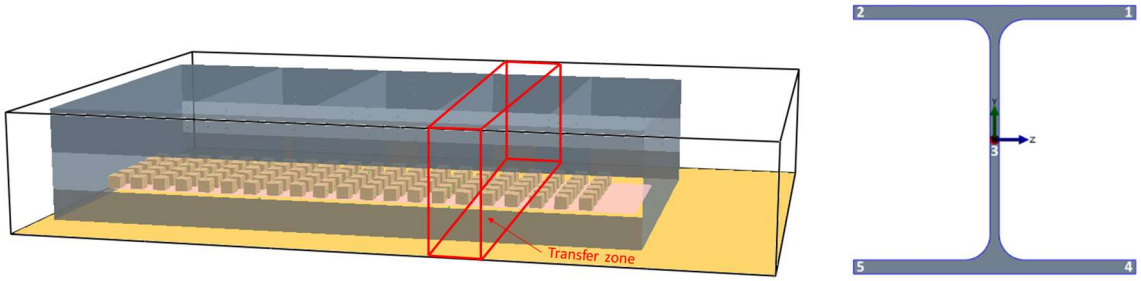

Figure 4 – (a) FDS model for the fire test n°2 with the transfer zone for SAFIR highlighted ; (b) Location of the five points of interest for steel temperature in SAFIR

3.3 Fire spread and heat release rate

All the faces of each cube, except the ones facing the floor, are set as burning surfaces. Heat release rate per unit area curves are predefined and assigned to these burning faces. The spread mechanism is governed by planar devices placed on each burning face to measure the temperatures on the solid surfaces. In FDS, quantitative results can be obtained through the use of devices, evaluated using cell centered or face centered values of the cell the device is located in. Devices on solid surfaces allow prescribing a solid phase quantity, and they can be coupled with a spatial statistics option (in which case the output quantity is not associated with just a single point on the surface). The spatial statistics option MAX was used, and caused FDS to

write out the maximum value of the surface temperature over the cells that are included in the specified bounded volume (Charlier *et al.*, 2020). If the latter reaches 250°C on at least one face of the cube, then all five burning faces are set to ignite and follow the prescribed heat release rate per unit area (HRRPUA) curve. This ignition temperature was chosen based upon cone calorimeter testing which found a critical heat flux for ignition of c. 13 kW/m^2. The RAMP function describing the evolution of HRRPUA with time, presents a symmetric profile: a growing phase, a plateau, a peak, a plateau and finally a decay phase. For sake of clarity, the HRRPUA parameter is redefined here via two parameters: HRRPUA_floor refers to the heat release rate per unit area of floor, while HRRPUA_assigned refers to the heat release rate per unit area of burning faces. The calibrated model has a plateau HRRPUA_floor equal to 250 kW/m^2 (corresponding to HRRPUA_assigned equal to 217 kW/m^2) and a peak HRRPUA_floor equal to 500 kW/m^2 (corresponding to HRRPUA_assigned equal to 434 kW/m^2). Indeed, the fire load consists of 21 columns and 6 rows of cubes (i.e. a total burning surface of 64.5 m^2) placed on a floor area of 56 m^2. The surface below the RAMP function (and indirectly the duration of this function) can be evaluated from a given HRRPUA and a given fire load. In the experimental campaign, a fire load of 511 MJ/m^2, representative of an office building according to EN1991-1-2, was set up.

4. Calibration of the fire tests – gas temperatures

4.1 Procedure

Gas temperatures in the test compartment were recorded at different locations using thermocouples. This section focuses on thermocouple trees TRL4 to TRL8, placed within the central zones along the length of the compartment, between gridlines B and C, as depicted on Figure 1. The first thermocouple tree (TRL4) is positioned at 2.5m from the back wall (gridline 1), i.e. at 1.5 m from the source of ignition. These thermocouple trees are equidistant, with 2.5m between each of them. Each tree was equipped with thermocouples provided at six different levels: at 0.5 m (Level 1), at 1 m (Level 2), at 1.5 m (Level 3), at 2 m (Level 4), at 2.5 m (Level 5) and at 2.7 m (Level 6) from the floor. The gas temperatures measured through the thermocouples are compared with FDS output 'THERMOCOUPLE' which is the temperature of a modelled thermocouple (with bead size set to 1.5mm as in the experimental campaign).

4.2 Comparison of gas temperatures

The graphs from Figure 5 to Figure 7 present the gas temperatures measured during test n°1 and the ones resulting from FDS, while the graphs from Figure 8 to Figure 10 present the gas

temperatures measured during test n°2 and the ones resulting from FDS. It can be observed that the global fire spread is well captured, as well as main tendency in terms of temperatures. Note that the temperatures generated by FDS for lower levels are higher than the ones measured, while the temperatures generated by FDS for middle and upper levels are closed to the ones measured. For level 2: the FDS temperature profiles present sharp growing and sharp decaying phases, while for levels 4 and 6 the FDS temperature profiles present first a smooth growing phase before a second sharp growth, then a sharp decay, followed by another smooth decaying phase. This corresponds to what was measured during the test and can be explained by the hot gases developing at the upper part of the compartment. Nevertheless, the FDS model is not able to capture the different temperature profile of TRL4 and TRL5, as well as the small acceleration which can be seen from the test curves TRL6, TRL7 and TRL8 being a bit closer in time. It has to be noted that the FDS results corresponding to TRL8 provide lower temperatures than other TRLs, which can be explained by the fire plume shape, which leans backwards due to air entrainment from the open end of the compartment. This methodology is not aimed at performing detailed analysis of the fire itself: it is aimed at evaluating the heating of the structural elements of the compartment to, in the end, evaluate the mechanical behavior of the structure subjected to travelling (or spreading) fire. Gas temperatures therefore represent an intermediate result to the steel temperatures, the topic of the next section.

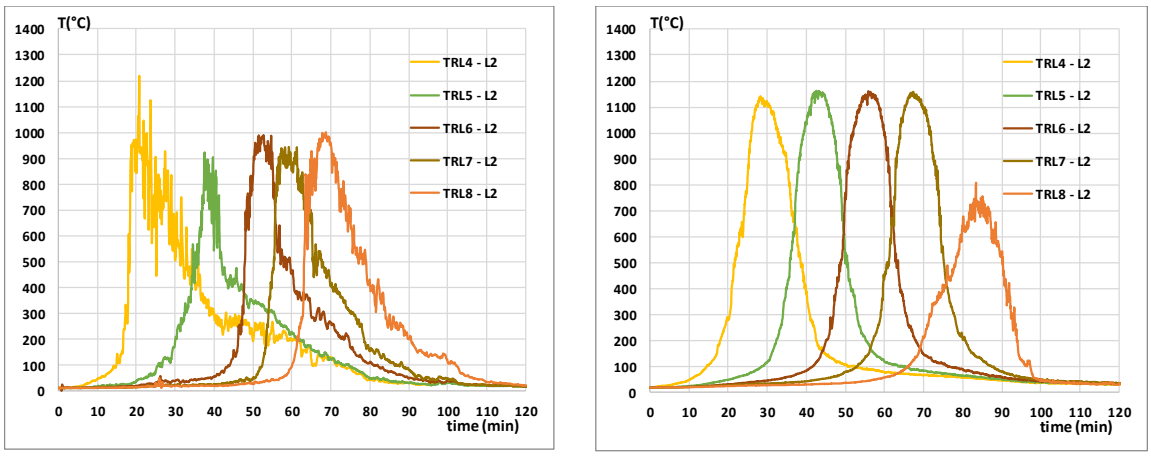

Figure 5. Comparison of gas temperatures for test n°1 at Level 2 (a) test measurements; (b) FDS results

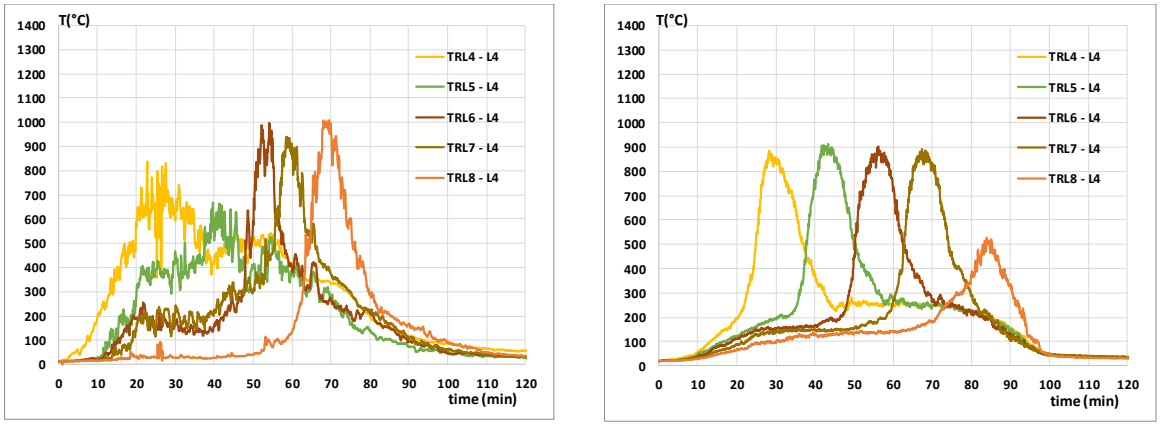

Figure 6. Comparison of gas temperatures for test n°1 at Level 4 (a) test measurements; (b) FDS results

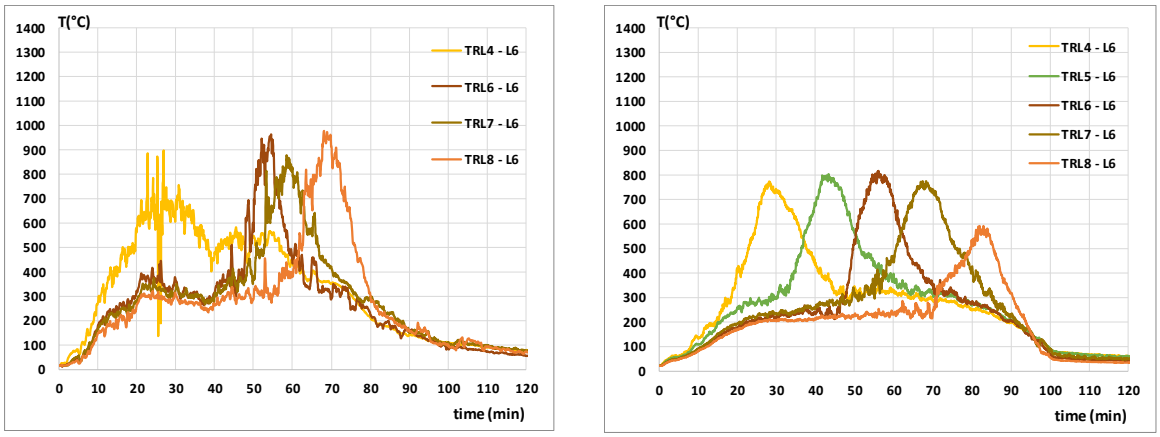

Figure 7. Comparison of gas temperatures for test n°1 at Level 6 (a) test measurements; (b) FDS results

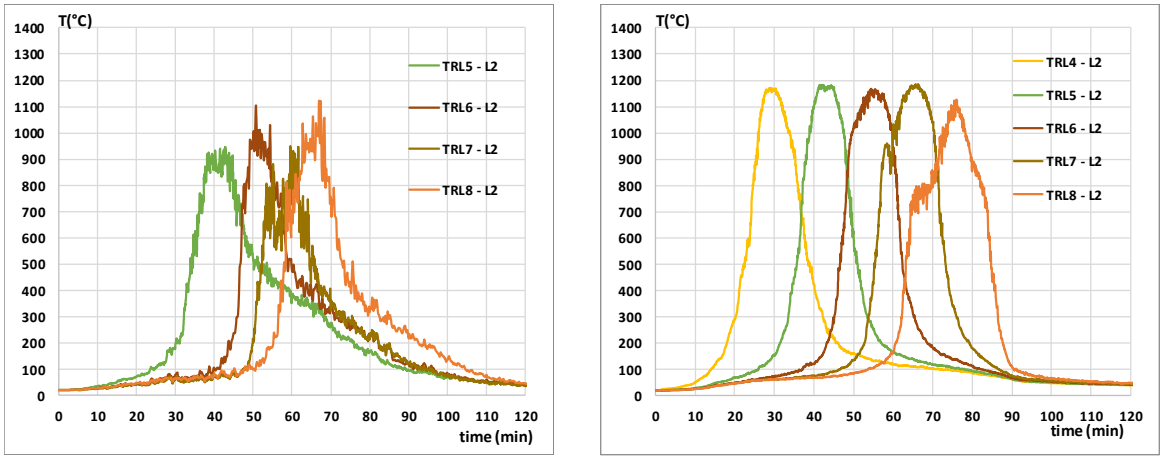

Figure 8. Comparison of gas temperatures for test n°2 at Level 2 (a) test measurements; (b) FDS results

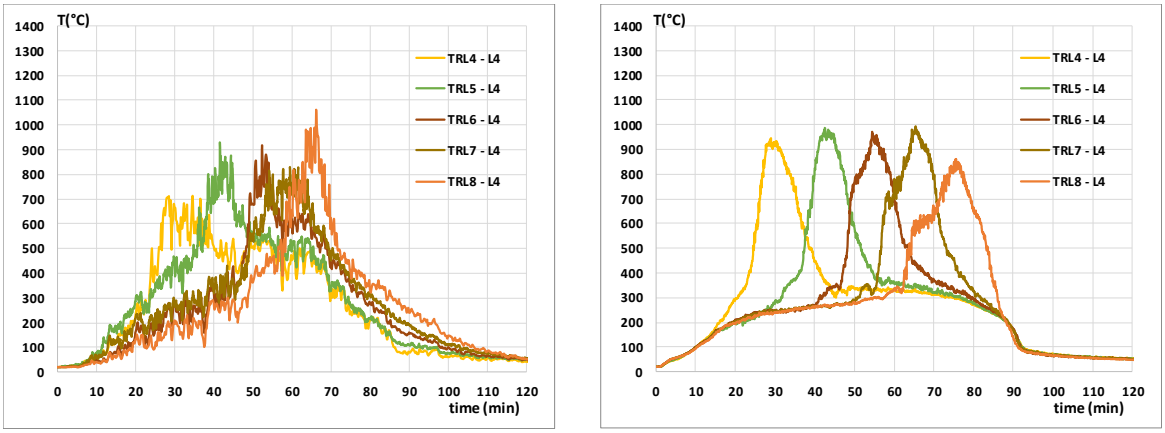

Figure 9. Comparison of gas temperatures for test n°2 at Level 4 (a) test measurements; (b) FDS results

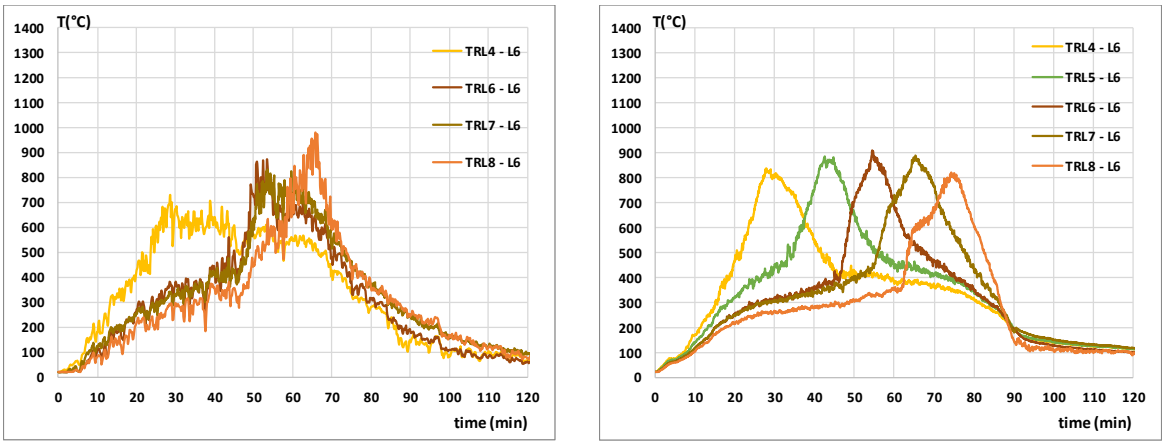

Figure 10. Comparison of gas temperatures for test n°2 at Level 6 (a) test measurements; (b) FDS results

5. Calibration of the fire tests – Steel temperatures

5.1 Assessment of steel temperatures through the use of EN1993-1-2

The steel temperatures comparison is performed for the unprotected steel column (hot rolled profile HE 200 A) positioned just next to the thermocouple tree TRL7, whose location is highlighted on Figure 1. Three thermocouples were provided at five levels along the height of the column: at the same heights as the gas thermocouples but omitting level 6. All thermocouples were provided at 3 mm depth from the surface of the flanges and the steel web, on parts of the column facing the source of ignition. The thermocouples provided in the web were positioned in the middle while the thermocouples provided in the flanges were at 20 mm distance from their edges. This experimental data is compared with numerical results using two different methods. In a first simplified step, the CFD output 'THERMOCOUPLE' was used to

evaluate the related steel temperature using the incremental formula from EN1993-1-2 (CEN, 2005). This method considers a constant temperature through a given section (i.e. at a given height). In a second and more complex step, a coupling between CFD (FDS software) and FE (SAFIR® software version 2019b0 (Franssen and Gernay, 2017)) was used. Radiative intensities and gas temperatures calculated by FDS have been used by SAFIR® to calculate the temperatures in the steel column. This coupling generates a non-uniform temperature distribution across the different sections of the steel column.

The steel temperature of a structural element can be obtained, in a simplified manner, from the incremental formula from EN1993-1-2 section 4.2.5.1 providing the increase of temperature $\Delta\theta_{a,t}$ in an unprotected steel member during a time interval Δt, see equation (1). The unprotected column is a hot rolled steel profile HE 200 A, therefore having a section factor of 211m^{-1}, and the correction factor for the shadow effect was considered equal to 1. The temperature is calculated for a column corresponding to the TRL7 position, at five heights: Level 1 to Level 5. The analysis was carried out using the FDS outputs 'THERMOCOUPLE'. These results accommodate the radiation effect, which is evaluated from all direction as the thermocouple is modelled as a sphere. They also consider the convective exchange with environment gas.

$$\Delta\theta_{a,t} = k_{sh} \frac{A_m/V}{c_a \rho_a} \dot{h}_{net} \Delta t \quad (1)$$

Where k_{sh} is the correction factor for the shadow effect [-];
A_m/V is the section factor for unprotected steel elements [1/m];
A_m is the surface area of the member per unit length [m^2/m];
V is the volume of the member per unit length [m^3/m];
c_a it is the specific heat of steel[J/kgK];
$\dot{h}_{net}$ is the design value of the net heat flux per unit area [W/m^2];
Δt is the time interval [s];
ρ_a is the unit mass of steel [kg/m^3].

5.2 Assessment of steel temperatures through coupling CFD and FEM

The steel temperature of a structural element can be also obtained while coupling CFD and FEM, using the FDS simulation results as inputs for subsequent thermal and mechanical SAFIR simulation. When launching the FDS simulation, a specific command is introduced to request

the creation of a transfer file in which gas temperatures, coefficients of convection and radiation intensities are written to be used by the subsequent FEM analysis by SAFIR (Tondini *et al.*, 2016). Indeed, the FDS command RADF allows to save the radiation intensities I_{ijk}^{l}, for each cell with indices ijk that is bounded by the transfer zone and for each solid angle l (McGrattan *et al.,* 2017). Linear interpolations are performed by SAFIR when reading the transfer file to compute the relevant values at the requested positions in time and in space. Using this data as input, a series of 2D transient thermal analyses are performed along the structural members and the results are stored in appropriate files. A temperature distribution is calculated for each longitudinal point of integration of each beam finite element. In this case, two points of Gauss are defined along the BEAM elements. The coupled code has previously been verified in relation to an open car park (Tondini *et al*., 2016) and to a steel rack system to be placed next to a pool fire (Tondini *et al*., 2012). In these 2D thermal analyses, the impinging flux is computed for each boundary (in the sense of finite element discretization) of the section, depending on its orientation. A hypothesis that was present in SAFIR versions prior to 2019b0 was that, when computing temperatures in a beam section or a shell section heated by a CFD fire, the flux at the different boundaries of the section was calculated at the position of the node line (for beams) or at mid-level of the shell (for shell elements), for all boundaries of the section. As of version 2019b0, the flux is computed at the precise position of the boundary, for each boundary of the section. For the boundaries on concave parts of the section, impinging radiative intensities from certain directions are discarded if there is an obstruction by other parts of the section, but mutual radiation between different boundaries of the section in the concave regions is not considered.

The zone for which a transfer file is created in highlighted in Figure 4 (a). This zone covers the full width of the CFD domain and a portion of 1.6 m of its length. The upper coordinate (in height) of this zone was set equal to the height of the lower face of the ceiling, to avoid enclosing in the thermal analysis the colder temperatures from the concrete ceiling. Generally, in the CFD model, the dimensions of a rectangular compartment correspond to the clear distances between opposite walls. However, in the FE model, a slab is generally modelled in correspondence to its centreline. Thus, the slab would fall outside the CFD domain, and assumptions have to be made to determine thermal information at the slab centreline (Charlier et al., 2020). In this paper, the slab was not comprised in the transfer zone. The column is divided into 17 BEAM elements of the same length (0.16m) and two integration points are defined per BEAM element. Since the temperatures are computed at each integration point, the

heights at which SAFIR provides results slightly differ from the heights at which steel temperatures were measured during the test (maximum discrepancy of 5 cm). The evolution of the steel temperatures resulting from the SAFIR analysis presented below derives from the average of the steel temperatures computed in 5 points, in flanges: points 1, 2, 4, 5 and in the web: point 3, as highlighted in Figure 4 (b).

Figure 11 provides the evolution of the steel temperatures across the section located at level 5, as a function of time and at the five points of interest highlighted in Figure 4 (b). From the start of the fire until around 40 minutes: steel temperatures are below 200°C and all five curves follow a similar evolution. From around 40 minutes until around 70 minutes: steel temperatures increase to around 650°C. From around 70 minutes until around 90 minutes: steel temperatures decay to around 300°C. The same information is provided in Figure 11 for test n°2: from the start of the fire until around 50 minutes: steel temperatures are below around 300°C and all five curves follow a similar evolution. From around 50 minutes until around 67 minutes: steel temperatures rise up to around 750°C. From around 67 minutes until around 90 minutes: steel temperatures decay to around 300°C. For both tests, during the sharply growing phase: points n°2, 3 and 5 heat slightly faster, as these points corresponds to the left part of the profile (facing gridline 1), and during the decay phase points n°2 and 5 cool slightly faster. The mesh within each section can be seen on Figure 13: two finite elements are defined across the width of the flanges and of the web. Figure 13 (a) and (b) depicts the steel temperature distribution obtained across the section located at level 5 with SAFIR at 50 minutes and 80 minutes, respectively. At 50 minutes (i.e. before the temperatures peak), a gradient can be observed in the flanges from left (higher steel temperatures towards gridline 1) to right (lower temperatures towards gridline 4). At 80 minutes, the reverse effect can be observed (i.e. higher steel temperatures towards gridline 4), and this reflects the spread of the fire in the compartment from left to right. Globally, the temperatures at the five points of interest present a similar evolution, the temperature gradient within the section being quite limited, and the same tendency is observed for the different levels of the column. The evolution of the steel temperatures resulting from the SAFIR analysis shown below will therefore be presented as the average of the steel temperatures from the five points of interest.

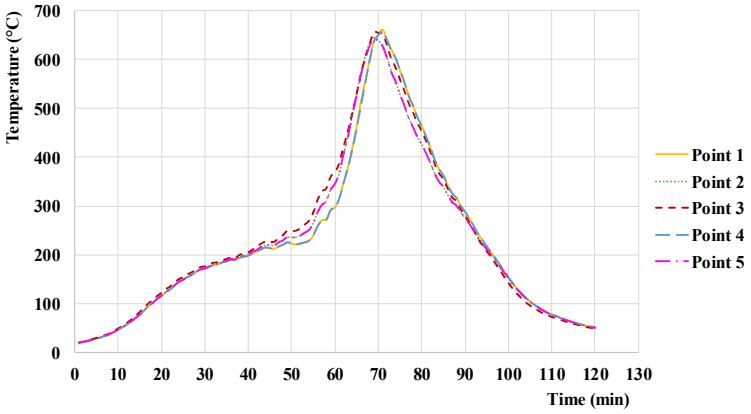

Figure 11. Steel temperatures evolution in test n°1 at level 5 from SAFIR at different locations of the section

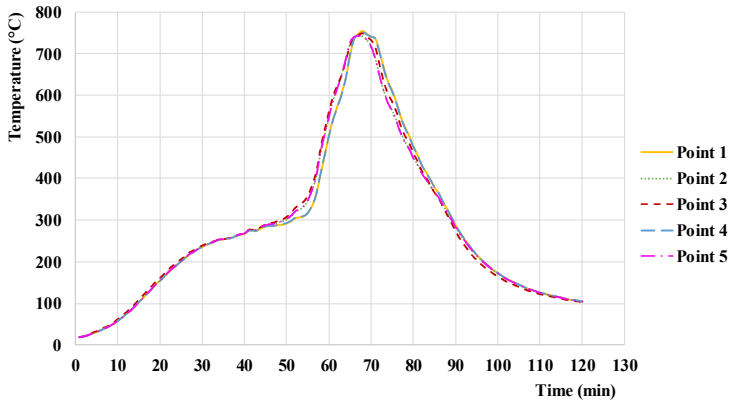

Figure 12. Steel temperatures evolution in test n°2 at level 5 from SAFIR at different locations of the section

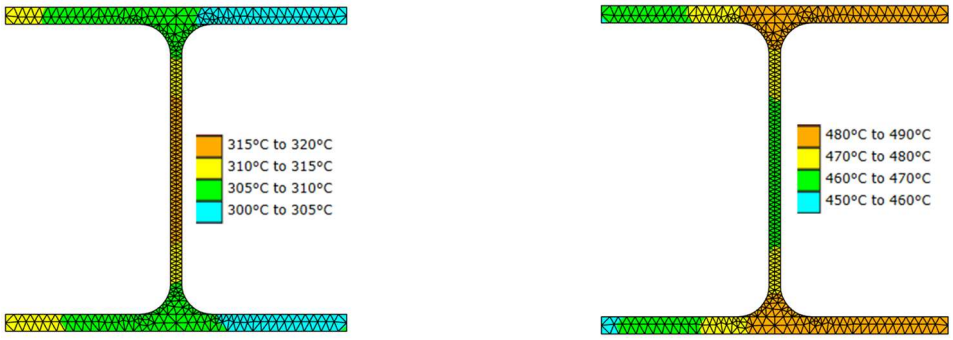

Figure 13. Steel temperature distribution in test n°2 across the section located at level 5 at (a) 50 minutes; (b) 80 minutes; (c) Steel temperatures evolution at level 5 from SAFIR at different locations of the section

5.3 Comparison of steel temperatures

The Figure 14 and Figure 15 present the steel temperatures in column close to TRL7 during test n°1, from level 2 (1 m from the floor level) to level 5 (2,5 m from the floor level). Similarly, the Figure 16 and Figure 17 present the steel temperatures in column close to TRL7 during test n°2. The following results are presented: steel temperatures directly measured during the test ("TEST – measure"), the steel temperatures evaluated considering the FDS output from "thermocouple devices" and applying the formula from EN1993-1-1 ("FDS tmc – via EC3")

and the steel temperatures computed by SAFIR, using the radiation intensities from FDS as input ("SAFIR"). The results obtained through coupling FDS and SAFIR are quite similar to the ones obtained through the application of the EN1993-1-1 formula, the main difference being the maximum temperatures (the temperatures obtained via FDS-SAFIR are lower and closer to the ones measured during the test). The following conclusions can be brought (comparing the measured temperatures with the ones obtained with FDS-SAFIR):

- Steel temperatures from lower levels are too high in comparison to the ones of the test (the results for level 1 are not shown but the tendency is similar to the one at level 2);
- Steel temperatures from higher levels (from level 3 to level 5) show a very good correspondence with the ones of the test. For test n°1, they are nevertheless a bit cooler – around 80°C - at level 5. This is not the case for test n°2;
- The global profile versus time is well captured;
- There is an important difference in the descending branch: the ones obtained numerically being sharper than the ones measured. This could be explained by FDS's inability to properly capture glowing embers as well as the heat accumulated within the compartment.

The fact that temperatures are too high at lower levels (close to the cubes) can be explained by the simplified representation of the fire load. With the wood cubes, it is prescribed that the heat is released at each cube's exterior, while in reality (continuous wood crib) some burning sticks are hidden by other sticks, implying that some heat is contained inside the crib and not radiated externally.

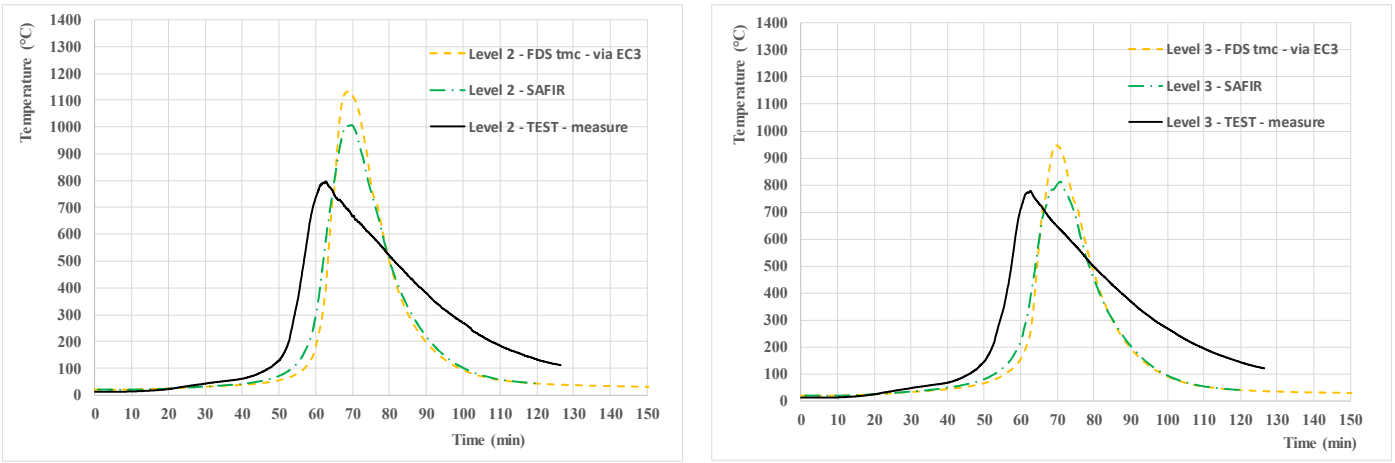

Figure 14. Steel temperatures in column close to TRL7 during test n°1 (a) at level 2; (b) at level 3

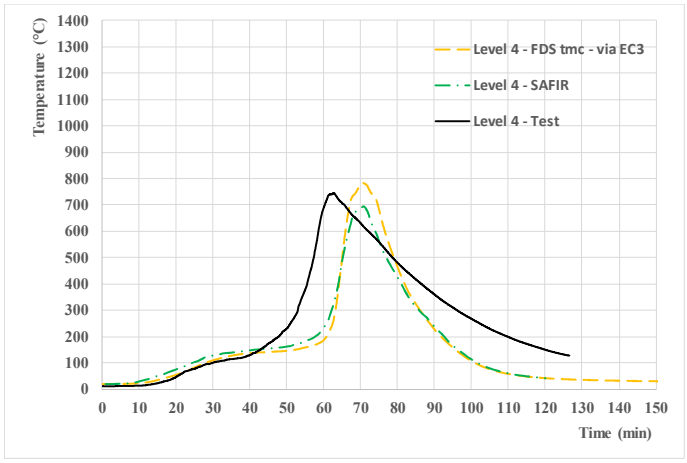

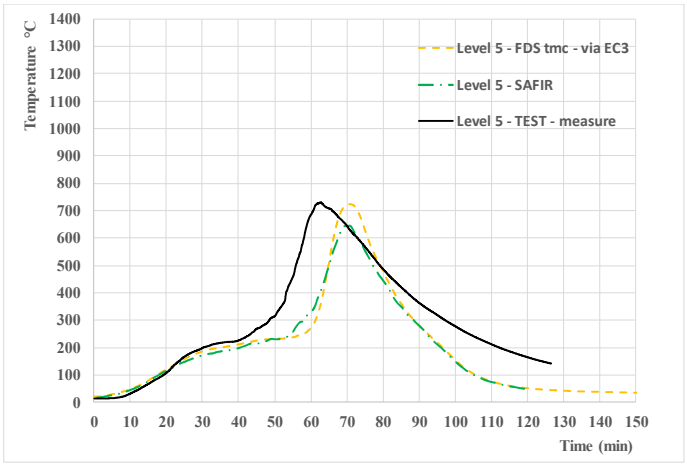

Figure 15. Steel temperatures in column close to TRL7 during test n°1 (a) at level 4; (b) at level 5

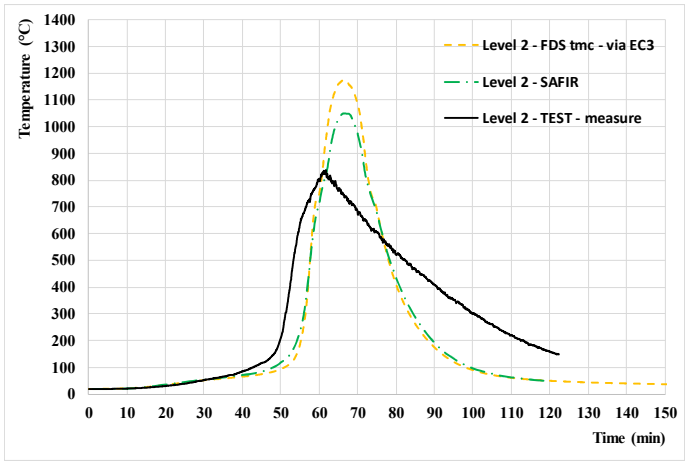

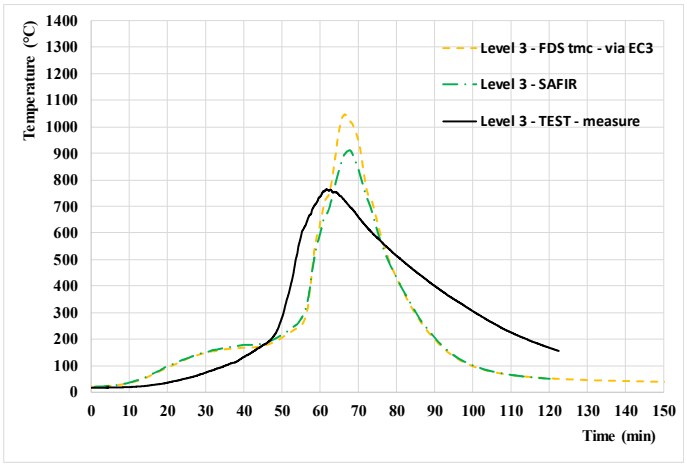

Figure 16. Steel temperatures in column close to TRL7 during test n°2 (a) at level 2 ; (b) at level 3

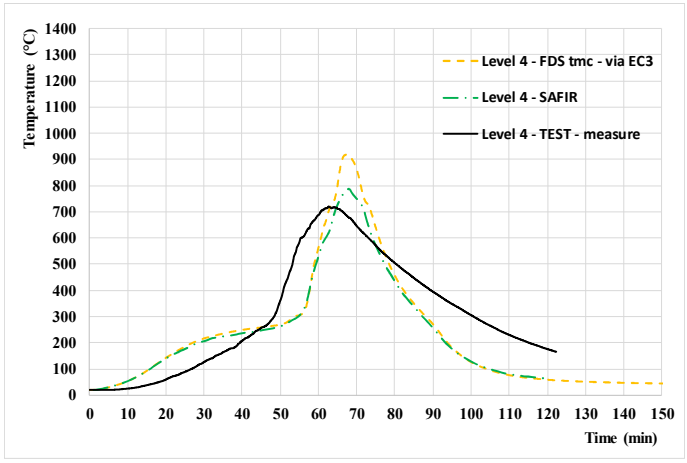

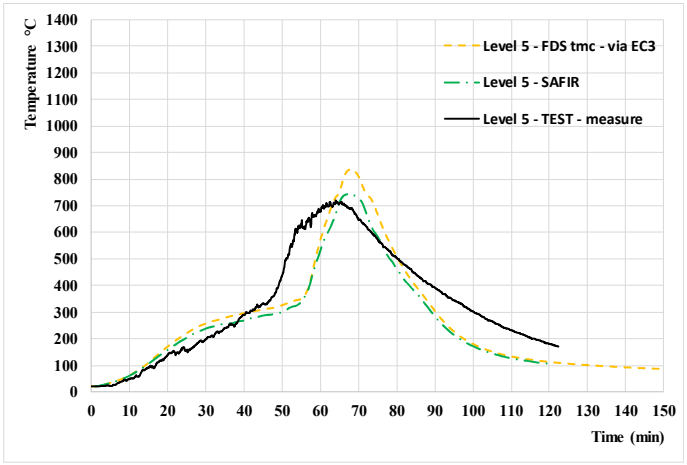

Figure 17. Steel temperatures in column close to TRL7 during test n°2 (a) at level 4; (b) at level 5

6. Discussion

The methodology used for the representation of burning fuel has some limitations. Before a cell reaches the ignition temperature, its heating is computed while considering heat exchanges with the environment. But as soon as the ignition temperature is met, FDS represents the fire by releasing volatile combustibles which, if all are burnt, results in the prescribed HRR curve. This is done without considering the evolution of heat exchange with the environment. Moreover, the simplified representation of the fire load using discrete cubes prevents air to flow through the objects, and implies heat being released at each cube's exterior instead of at each stick's boundary. This limitation has shown consequences on the temperatures computed within or just next to the burning cubes, these being too high in comparison with the experimental ones. Finally, it also leads to a non-negligible difference in the steel temperature descending branch, which could be explained by the CFD model's inability to properly capture glowing embers as well as the heat accumulated within the compartment, and such aspects could be improved in future research.

The authors would like to point out that this methodology is not aimed at performing detailed analysis of the fire itself – it is aimed at evaluating the structural response (i.e. heating of the structural elements, followed by a mechanical analysis) in a compartment subjected to travelling fire (or spreading fire) at the global level. Although it implies some simplifications, the proposed approach can allow for both an acceptable representation of the travelling fire in terms of fire spread and steel temperatures while being less computationally demanding than modelling the exact geometry of the fire load (the CFD simulations detailed in this paper required 36.9 and 41.6 hours to complete for test n°1 and n°2 respectively), making it more desirable for practical applications.

7. Conclusion

This paper presents a simplified representation of the fire load for travelling fire development using CFD analyses with FDS software. The potential benefit of such representation is shown while modelling two of the three TRAFIR natural fire tests and comparing gas temperatures measured at mid-width, along the length of the compartment and steel temperatures measured on a central steel column. The steel temperatures resulting from the CFD model were evaluated using two methods: one based on the incremental formula from EN1993-1-2 and other one linking CFD (FDS software) and FEM (SAFIR® software). The results obtained through these two methods are quite similar, the main difference being the maximum temperatures: the temperatures obtained via FDS-SAFIR are closer to the ones measured during the test. The

steel temperature profiles globally showed a good correspondence with the ones of the test but with the following limitations: too high steel temperatures in the vicinity of the fuel and an underestimated descending branch. This work has revealed, within the limits of the modelled compartments, that the proposed simplified representation of the fire load appears to be appropriate to evaluate the temperature of steel structural elements. This paper also presents the first comparisons of FDS-SAFIR coupling with experimental results, highlighting promising outcomes.

This simplified fire load representation, as well as the described FDS-SAFIR coupling, could be used by design offices for practical applications (evaluating the structural response in a compartment subjected to travelling or spreading fire at the global level) and for future research concerning compartments subjected to travelling fire (or spreading fire). In the frame of the same research project TRAFIR, this simplified fire load representation is also used in parametric analyses performed to reproduce a broader range of scenarios encompassing different geometries, fires and end-use situations, so as to generate an extended virtual experimental dataset.

References

- CEN (European Committee for Standardization) (2002), "EN 1991-1-2: Eurocode 1: Actions on structures – Part 1-2: General actions – Actions on structures exposed to fire", Brussels, Belgium.
- CEN (European Committee for Standardization) (2005), "EN 1993-1-2: Eurocode 3: Design of steel structures - Part 1-2: General rules - Structural fire design", Brussels, Belgium.
- Charlier, M., Gamba, A., Dai, X., Welch, S., Vassart, O., Franssen, J.-M. (2018), "CFD analyses used to evaluate the influence of compartment geometry on the possibility of development of a travelling fire", *Proceedings of the 10th International Conference on Structures in Fire (Ulster University, Belfast, UK)*, pp.341-348.
- Charlier, M., Gamba, A., Dai, X., Welch, S., Vassart, O., Franssen, J.-M. (2020), "Influence of compartment geometry on travelling fires using CFD and FE software", *Structures and Buildings Themed issue 'Structural design for fire safety' (accepted for publication in 2020, DOI: 10.1680/jstbu.20.00037)*.
- Degler, J., Eliasson, A., Anderson, J., Lange, D., Rush, D. (2015), "A-priori modelling of the Tisova fire test as input to the experimental work", *Proceedings of the 1rst International Conference on Structural Safety under Fire & Blast (Glasgow, UK)*.
- Franssen, J.-M., Gernay, T. (2017), "Modeling structures in fire with SAFIR®: Theoretical background and capabilities", *Journal of Structural Fire Engineering 8(3)*, pp.300-323.
- Franssen, J.-M., Gamba, A., Charlier, M. (2019), "Toward a standardized uniformly distributed cellulosic fire load", *Proceedings of the 3rd International Fire Safety Symposium (Ottawa, Canada)*.
- Gamba, A., Charlier, M., Franssen, J.-M. (2020), "Propagation tests with uniformly distributed cellulosic fire load", *Fire Safety Journal 117*, 103213.
- Horová, K. (2015), "Modelling of Fire Spread in Structural Fire Engineering", PhD thesis, Czech Technical University in Prague.
- McGrattan, K., Hostikka, S., McDermott, R., Floyd, J., Weinschenk, C., Overholt, K. (2017), "Fire Dynamics Simulator User's Guide", Sixth Edit. National Institute of Standards and Technology (NIST), Special Publication 1019.

- Nadjai, A., Alam, N., Charlier, M., Vassart, O., Dai, X., Franssen, J.-M., Sjöström, J. (2020), "Travelling fire in full scale experimental building subjected to open ventilation conditions", Accepted for the 11th Intl. Conf. on Structures in Fire.
- Rush, D., Lange, D., Maclean, J., Rackauskaite, E. (2016), "Modelling the thermal and structural performance of a concrete column exposed to a travelling fire – Tisova Fire Test", *Proceedings of the 9th International Conference on Structures in Fire*, pp.110-118.
- SFPE Handbook of Fire Protection Engineering (2002), Third Edition, NFPA.
- Tondini, N., Vassart, O., Franssen, J.-M. (2012), "Development of an interface between CFD and FE software", *Proceedings of the 7th International Conference on Structures in Fire (Zurich, Switzerland)*.
- Tondini, N., Morbioli, A., Vassart, O., Lechêne, S., Franssen, J.-M. (2016), "An integrated modelling strategy between a CFD and an FE software: Methodology and application to compartment fires", *Journal of Structural Fire Engineering 7(3)*, pp.217-233.
- Wald, F., Jána, T., Horová, K. (2011), "Design of Joints to Composite Columns for Improved Fire Robustness: To Demonstration Fire Tests", Czech Technical University in Prague.
- Welch, S., Miles, S., Kumar, S., Lemaire, T. and Chan, A., (2008), "FIRESTRUC - Integrating advanced three-dimensional modelling methodologies for predicting thermo-mechanical behaviour of steel and composite structures subjected to natural fires", in Karlsson, B. (Ed.), *Fire Safety Science - Proceedings of the Ninth International Symposium, International Association for Fire Safety Science, Reykjavik*, pp.1315-1326.
- Wickström, U., Duthinh, D., McGrattan, K., (2007), "Adiabatic Surface Temperature for Calculating Heat Transfer to Fire Exposed Structures", *Proceedings of the 7th International Interflam Conference*, London, UK.
- Yang, P.-Y. (2016) "Computational modelling of fire spread in a full-scale compartment fire test", IMFSE thesis, School of Engineering, University of Edinburgh.